Direct Interelectrode Tunneling in GaSe†

S. L. Kurtin,* T. C. McGill,‡ and C. A. Mead
California Institute of Technology, Pasadena, California 91109
(Received 13 January 1971)

Using thin films of the layer compound gallium selenide, we have fabricated experimental structures which are nearly ideal for the study of tunneling currents. All of the parameters relevant to current flow in these structures can be independently determined since single-crystal gallium selenide films have the properties of the bulk material and also well-defined interfaces. A new analytical technique for determining the energy-momentum dispersion relation within the forbidden gap of a solid is discussed and applied to current-voltage data obtained from metal-GaSe-metal structures. The resulting E-k relation is shown to be an intrinsic property of GaSe. Tunneling currents in GaSe are shown to be quantitatively understood in terms of this E-k relation, the geometry of a given structure, and a simple model of current flow via tunneling.

I. INTRODUCTION

Although the basic concepts of tunneling are firmly rooted in the early quantum mechanics,[1] only recently has progress been made in gaining a quantitative understanding of tunneling in solids.[2] Perhaps the greatest impediment has been the experimental problems associated with the fabrication of suitable structures.

Since the probability amplitude of a tunneling electron is exponentially damped in space,[3] the "forbidden" region through which tunneling is to occur must be extremely thin (< 100 Å) to favor tunneling over other current-flow mechanisms. It has not in general been possible to cleave single-crystal solids into films this thin and hence other techniques of fabricating a thin forbidden region are traditionally employed. Perhaps the best known technique is the controlled oxidation[4] of a metal, followed by vacuum deposition of counter electrodes, thus forming metal-insulator-metal (MIM) structures. Early studies[5-7] of direct interelectrode tunneling in solids were conducted using structures fabricated by this or similar techniques. It was observed that currents flowing in such structures were often temperature independent and exhibited a nearly Ohmic dependence on applied voltage for small applied voltages. This sort of behavior is in qualitative agreement with the predictions of simple tunneling theory. However, when attempts were made to obtain quantitative agreement between theory and experiment, perplexing discrepancies arose.

The theoretical model first applied to tunneling in MIM structures[8] dealt explicitly with a symmetric barrier potential; the forbidden region within this potential was assumed to behave like a vacuum (except for a dielectric constant different from unity). In many cases the gross differences between theory and experiment could be minimized by using an "effective thickness" for the insulating film or an "effective mass" for the tunneling electron. These parameters were chosen specifically to bring theory and experiment into agreement, could not be independently determined, and bore little relation to the actual parameters of the structure under study. Although this approach served as a convenient method for classifying experimental data, it did not provide a deep understanding of tunneling, or even unequivocal evidence that tunneling was indeed being observed.

Of course, it was realized that the chemical composition of the grown insulating film was not uniform, and that the metal-oxide interface was in all likelihood far from the idealized rectangular barrier shape usually assumed. In fact, nonsymmetric current-voltage curves were often observed for nominally symmetric structures (e.g., Al-Al_2O_3-Al). The extent to which these difficulties invalidated the model was not clear, and hence fundamental inadequacies in the model went unnoticed. A large stride toward overcoming the major experimental difficulties was taken by McColl *et al.*[9] in the study of thin mica films cleaved from bulk crystals. Despite crystal-to-crystal variation, great consistency was observed in all measurements obtained on structures fabricated from a given initial bulk crystal. Parameters required to describe tunneling currents in thin mica films were in good agreement with the corresponding independently measured properties of the bulk mica. Yet, certain problems remained, including an apparent systematic deviation between theory and experiment. Careful analysis of the data indicated that characterizing the quantum mechanically forbidden region as if it were a simple vacuum was probably a misleading oversimplification.

A successful approach toward the resolution of this theoretical/experimental problem was taken by Lewicki and Mead[10,11] who studied current flow in

thin amorphous films of aluminum nitride (formed by plasma discharge nitriding). Working with Stratton,[12] they recognized the importance of the E-k dispersion relation within the forbidden gap in describing tunneling through solids, and were able to piece together an E-k relation for AlN by measuring the thickness dependence of the tunneling probability at several values of applied bias. This experimentally determined E-k relation successfully described many of the tunneling phenomena observed in AlN thin films.

In this paper we report a synthesis and extension of the previously described techniques. By choosing to study thin films of the layer compound gallium selenide, we can fabricate nearly ideal structures. All of the parameters relevant to current flow in these structures can be determined by independent experiments. The thin gallium selenide film under study is single crystal in character and therefore has the properties of bulk material and also well-defined interfaces. An improved analytical technique for determining the energy-momentum dispersion relation within the forbidden gap of a solid (from appropriate current-voltage measurements) is discussed and applied to data obtained from metal-GaSe-metal structures. The resulting E-k relation is shown to be an intrinsic property of GaSe. Tunneling currents in GaSe can thus be quantitatively understood in terms of this E-k relation, the independently determined parameters of a given structure, and a simple model of current flow via tunneling.

II. THEORY OF TUNNELING IN MIM STRUCTURES

Current flow arising from the direct tunneling of electrons from one metallic electrode to another through an intervening insulating layer provides a unique opportunity to study the quantum-mechanical interaction of electrons with solids. A tunneling electron interacts continuously with the solid through which transport is occurring; the details of this interaction can be unraveled only if a great deal of information about the experimental structure is available. Ideally, one seeks sufficient independent information about an experimental structure to construct an accurate (and hopefully simple) energy-band representation. The potential barrier through which tunneling is occurring should be well defined and experimentally controllable. Having satisfied these criteria, a straightforward model of tunneling can be constructed with some assurance that it is a reasonable representation of the physical situation. In the discussion that follows, we presume (and will, in fact, demonstrate in Sec. III) that these criteria are fulfilled for the metal-GaSe-metal structures discussed here, and that a simple trapezoidal barrier potential is appropriate.

Discussions of tunneling are often based upon the transfer Hamiltonian model.[2,13,14] In this description an idealized tunneling structure, as schematically illustrated in Fig. 1, is divided into three separate regions. For electrons with energies of interest, two of the regions are allowed (electrodes); the third region is unallowed (insulator). Current flow arises when there is a net transfer of electrons from one electrode to the other due to the interaction of the two electrodes through the insulator. This system is described by the quantum-mechanical Hamiltonian

$$H = H_L + H_R + H_T \,, \tag{2.1}$$

where H_L is the Hamiltonian for the left electrode (see Fig. 1), H_R is the Hamiltonian for the right electrode, and H_T (transfer Hamiltonian) contains the interaction between the two electrodes due to the insulating region. The transfer Hamiltonian may be expressed simply in terms of basis states $\{|\alpha\rangle\}$ and $\{|\beta\rangle\}$. The set $\{|\alpha\rangle\}$ is the set of single-particle solutions of the Hamiltonian for the left electrode and the insulating layer. These solutions decay into the right electrode. The set $\{|\beta\rangle\}$ is a similar set of functions for the right electrode. Using this basis, H_T is given by the expression

$$H_T = \sum_{\alpha,\beta} (M_{\alpha\beta}\, C_\alpha^\dagger C_\beta + M_{\alpha\beta}^*\, C_\beta^\dagger C_\alpha) \,, \tag{2.2}$$

where $M_{\alpha\beta} = i\hbar\, J_{\alpha\beta}(X_B)$ and $J_{\alpha\beta}\ (X_B)$ is the matrix element of the current operator between the states α and β integrated over plane S, parallel to the metal-insulator interface at some position X_B in the insulating layer.[13] That is,

$$J_{\alpha\beta}(X_B) = \int_S d\vec{S} \circ \vec{J}_{\alpha\beta}(X_B) \,, \tag{2.3}$$

where

$$\vec{J}_{\alpha\beta}(X_B) = \langle \alpha | \vec{J}(X_B) | \beta \rangle \,.$$

Application of Fermi's Golden Rule to compute the net rate of transfer produced by H_T gives

$$I(V) = 2\pi e\hbar \sum_{\alpha,\beta} |J_{\alpha\beta}|^2 [f_L(\epsilon_\alpha) - f_R(\epsilon_\beta)] \,, \tag{2.4}$$

where $I(V)$ is the current from left to right for an applied bias V; f_L and f_R are the Fermi factors for the left and right electrode, respectively; and ϵ_α and ϵ_β are the single-particle energies of the state α and the state β, respectively. In deriving Eq. (2.4), it is assumed that the electrodes are adequately described by a single-particle formalism.

Evaluation of the matrix element $J_{\alpha\beta}$ for direct tunneling in the standard way (see, for example, Refs. 2, 15–17) yields an expression for the current density

$$j(V)=\frac{2e}{h}\int dE\int\frac{d^2k_{11}}{(2\pi)^2}\,g(E,k_{11})[f_L(E)-f_R(E)]\exp\left(-2\int_{X_L}^{X_R}k(E,\vec{k}_{11},X)\,dX\right)\,, \tag{2.5}$$

where $\vec{k}_{11}$ is the parallel component of the wave vector of the electron in the electrode. It is important to note that the exponential factor which dominates this expression results from the exponential decay of the electronic wave function in the forbidden insulating region: $k(E,\vec{k}_{11},X)$ is the attenuation constant. For single-crystal insulators, k may be thought of, in band-structure terms, as the complex wave vector[18,19] within the forbidden gap. In general, $\vec{k}_{11}$ is a function of the electron energy E, the parallel component of the wave vector $\vec{k}_{11}$, and position in the insulator X. The dependence on X is due to the applied potential, and interface potentials which change the features of the band structure of the insulator relative to the electron's energy.

In Eq. (2.5), $g(E,\vec{k}_{11})$ is a pre-exponential factor which results from the matching of the wave functions at the interfaces. Its exact theoretical form will depend on the assumed boundary conditions. Attempts at experimentally verifying the form of $g(E,\vec{k}_{11})$ from structure in the bias dependence of the tunneling current have been unsuccessful.[15] Since k, the function of interest, is insensitive to the exact form or value of $g(E,\vec{k}_{11})$ we will take it to be unity. This approximation is equivalent to the usual WKB approximation.[2]

Further simplification of Eq. (2.5) can be realized by noting the rapid variation of the exponential factor with $\vec{k}_{11}$. This allows us to use the method of Laplace[20] to obtain a useful approximation for the integral. Taking the dependence of $k(E,\vec{k}_{11},X)$ on $\vec{k}_{11}^{\,2}$ to be given by

$$k(E,\vec{k}_{11},X)=[k^2(E,0,X)+k_{11}^2]^{1/2}\,, \tag{2.6}$$

we have

$$j(V)=\frac{e}{2\pi h}\int dE\,\left[\exp\left(-2\int_{X_L}^{X_R}k(E,0,X)\,dx\right)\Big/\int_{X_L}^{X_R}\frac{dx}{k(E,0,X)}\right][f_L(E)-f_R(E)]\,. \tag{2.7}$$

Since most tunneling experiments are performed at low temperature (to minimize thermionic currents), it is often a good approximation, and always theoretically handy, to take the temperature to be zero. This approximation makes sense if the natural width of the energy distribution of tunneling electrons is appreciably greater than the width added by the thermal tail on the Fermi distribution in the source electrode.[21]

There remains one useful simplification of (2.7) to be discussed. The energy E may be related to the spatial coordinate X such that k becomes a function of a single variable $\xi(X)$. This new variable $\xi(X)$ is the difference in energy between the conduction band and the energy of an electron located at X:

$$\xi(X)=\phi(X)-E\,. \tag{2.8}$$

Reexpressing $j(V)$ in terms of $\xi(X)$,

$$j(V)=\frac{e}{2\pi h}\int dE\exp\left(-2\int_{\xi(X_L)}^{\xi(X_R)}\frac{d\xi}{d\phi/dX}\,k(\xi)\right)\Big/\int_{\xi(X_L)}^{\xi(X_R)}\frac{d\xi}{(d\phi/dX)k(\xi)}\,. \tag{2.9}$$

This expression, although somewhat approximate, is of adequate precision and contains the basic physics of tunneling. A quantitative interpretation of experimental data using this expression requires $\phi(X)$ [and hence $\xi(X)$] be known independent of the measurement of tunneling currents.

Assuming now the trapezoidal barrier potential as shown in Fig. 1,

$$\phi(X)=\phi_1+(\phi_2-\phi_1-V)X/t\,, \tag{2.10}$$

and for an applied bias[22] in the range $-\phi_1<V<\phi_2$, Eq. (2.9) becomes

$$j(V)=\frac{e}{2\pi h}\int_0^V dE\exp\left(\frac{-2t}{\phi_2-\phi_1-V}\int_{\phi_1+E}^{\phi_2+E-V}d\xi\,k(\xi)\right)\Big/\int_{\phi_1+E}^{\phi_2+E-V}\frac{d\xi\,t}{(\phi_2-\phi_1-V)k(\xi)}\,. \tag{2.11}$$

This equation is a suitable basis for interpreting tunneling currents in structures known to have a trapezoidal barrier shape.

To interpret tunneling I-V characteristics in terms of $k(\xi)$ (i.e., the dispersion relation for the imaginary part of the wave vector) Eq. (2.11) must

be solved for $k(\xi)$, given $j(V)$ and the other parameters in the equation. For certain values of barrier energy and applied voltage, and for certain $k(\xi)$ functions, the distribution in energy of the tunneling electrons can be accurately approximated by a single sharp peak. In this case, expression (2.11) reduces to the familiar simple form[12] used by Stratton *et al.*, and the interpretation may be accomplished by simple mathematical manipulations. However, in general, Eq. (2.11) must be solved without simplifying approximations. Thus, one is faced with solving a nonlinear integral equation of the Volterra type of the first kind. Numerical solution is unavoidable.

Equations of the type given in Eq. (2.11) are usually solved by an adaptation of the well-known Newton's method for obtaining the roots of a system of nonlinear equations.[23] Basically, this technique consists of making an initial guess and then computing corrections to this guess from the integral equation. For example, let

$$\mathfrak{L}[j_{\text{expt}}(V),\, k(\xi)] = j_{\text{expt}}(V) - \frac{e}{2\pi h}\int_0^V dE \exp\left(-\frac{2t}{(\phi_2-\phi_1-V)}\int_{\phi_1+E}^{\phi_2+E-V} k(\xi)\,d\xi\right)\Big/\int_{\phi_1+E}^{\phi_2+E-V}\frac{d\xi}{k(\xi)}\,\frac{t}{(\phi_2-\phi_1-V)}, \quad (2.12)$$

where $j_{\text{expt}}(V)$ is the experimental current density as a function of bias and $\mathfrak{L}$ is a functional of both $j_{\text{expt}}(V)$ and $k(\xi)$. Obviously, $\mathfrak{L}$ will be identically zero when a solution is attained. Let $k_0(\xi)$ be the function which makes $\mathfrak{L}\equiv 0$, that is, $k_0(\xi)$ is the solution. In general, $k_0(\xi)$ is unknown. However, some initial guess at $k_0(\xi)$ is made. This guess $k(\xi)$ is related to $k_0(\xi)$ by the equation

$$k(\xi) = k_0(\xi) + \delta k(\xi)\,, \quad (2.13)$$

where $\delta k(\xi)$ is the correction required to make $k(\xi)$ equal $k_0(\xi)$. Substituting (2.13) into Eq. (2.12) and expanding in a Taylor's series about $k(\xi)$, we have

$$0 = \mathfrak{L}\{j_{\text{expt}}(V), k(\xi)\} + \int \frac{\delta}{\delta k(\xi)} \times \mathfrak{L}\{j_{\text{expt}}(V),\, k(\xi)\}\,\delta k(\xi)\,d\xi + \cdots\,, \quad (2.14)$$

where $\delta\mathfrak{L}/\delta k(\xi)$ is the functional derivative of $\mathfrak{L}$ with respect to $k(\xi)$. Neglecting higher-order terms in Eq. (2.14), this equation gives a value of $\delta k(\xi)$:

$$\delta k(\xi) = -\int dV\ \frac{\delta}{\delta k(\xi)} \times \mathfrak{L}^{-1}\{j_{\text{expt}}(V),\, k(\xi)\}\ \mathfrak{L}\{j_{\text{expt}}(V),\, k(\xi)\}, \quad (2.15)$$

where $\delta\mathfrak{L}^{-1}/\delta k(\xi)$, if it exists, is the inverse of the integral operator appearing in Eq. (2.14). Existence of the inverse determines that range of $j_{\text{expt}}(V)$ which is required to specify $\delta k(\xi)$ and $k_0(\xi)$ over a specific range of ξ. This point will be discussed in more detail below.

Evaluation of $\delta\mathfrak{L}/\delta k(\xi)$ may be accomplished by substituting $k(\xi)+\delta k(\xi)$ for $k(\xi)$ in Eq. (2.12) and expanding in $\delta k(\xi)$. The term linear in $\delta k(\xi)$ gives $\delta\mathfrak{L}/\delta k(\xi)$. The result of such a calculation is shown in Fig. 2, where the explicit dependence of $\delta\mathfrak{L}/\delta k(\xi)$ on V and ξ is shown. If the array in Fig. 2 is evaluated on a mesh in V and ξ with an equal number of points in ξ and V [as is done in the numerical solution of (2.13)], then one obtains a square matrix. If this matrix has a determinant which is different from zero, then the finite set of numerical equations which replace (2.13) has a unique solution. This condition determines the range of V which will give a unique set of values of k_0 on the mesh of ξ. Thus, it is possible to test the uniqueness of the calculated solution by computing the inverse of this matrix. While this method does not provide a rigorous mathematical test for uniqueness, it does suffice for the problem at hand.

Numerical solution proceeds in a straightforward manner.[17,24] Some difficulty is encountered in solving the linear equation (2.13) as a result of numerical instabilities. These difficulties may be overcome by the use of a powerful technique recently developed by Franklin for converting an ill-posed linear problem into a well-posed stochastic problem.[25]

III. EXPERIMENTAL CONSIDERATIONS

A. Gallium Selenide

Ideally one would like to take a well-characterized bulk insulator, cleave it into thin sections ($\leq$100 Å thick), and incorporate these thin sections into MIM structures. Such an approach is not usually feasible for a variety of practical reasons. There does not exist, however, a family of solids (the layer compounds) which is well suited to this approach.

Layer compounds are distinguished by their unusual crystallographic structure. Each layer (typically several atoms thick), is strongly bonded internally but only weakly bonded to its neighbors. Hence, thin single-crystal films can be obtained by pulling or peeling apart a macroscopic single crystal. This technique for fabricating well-defined MIM structures was pioneered by Foote and Kazan[26] and used by McColl in his study of current flow in thin films of mica.

Gallium selenide[27] is the particular layer

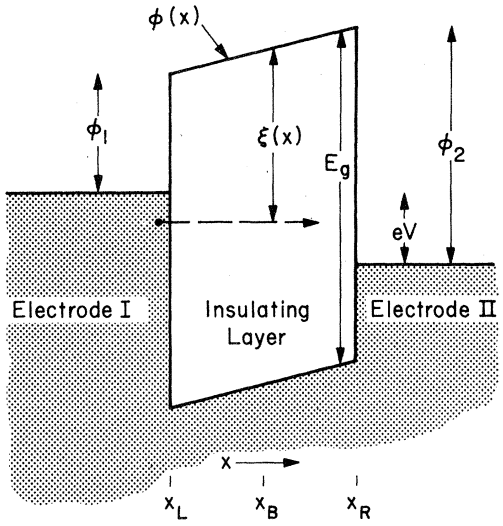

FIG. 1. Schematic energy-band representation of an ideal MIM tunneling structure in which electrode II is biased V volts with respect to electrode I. ϕ_1, ϕ_2 are metal-insulator barrier energies; $\phi(X)$ is the (trapezoidal) barrier potential; $\xi(X)$ is the energy of an electron tunneling from electrode I to electrode II, referenced to $\phi(X)$; the spatial coordinate X is used both as a continuous variable and to denote distinct regions of the structure.

semiconductor chosen for this study. GaSe was chosen because it is easy to work with, large single crystals can be easily grown by the modified Bridgeman technique, and prior experiments have well characterized the properties of bulk specimens. A previous study[28] of conduction mechanisms through somewhat thicker (~500 Å) GaSe films confirms the advantages of utilizing this material for the fabrication of thin-film MIM structures. That study provided an excellent example of contact-limited thermionic current flow. The quantitative agreement between theory and experiment which was observed is good evidence that the bulk and interface properties of GaSe are sufficiently well known to make a tunneling study worthwhile. The following are those properties[27,28] of our "as-grown" GaSe specimen which are relevent to tunneling currents in thin-film structures: band gap $E_g = 2.0$ eV; low-frequency dielectric constant $\epsilon_0 = 8$; optical dielectric constant $\epsilon_{opt} = 7$; Al-GaSe interface barrier energy $\phi_{Al} = 1.08$ eV; Au-GaSe interface barrier energy $\phi_{Au} = 0.52$ eV; Cu-GaSe interface barrier energy $\phi_{Cu} = 0.68$ eV; trap density $N_t < 10^{14}$/cm^3; carrier density at 300 °K $p \sim 3 \times 10^{14}$/cm^3.

B. Fabrication of MIM Structues

The technique by which MIM structures containing thin films of GaSe are fabricated is straightforward, but worthy of mention. Single-crystal films of GaSe, perhaps 10 μ thick, are peeled from a large boule and electroded on one side by vacuum-evaporating aluminum from a tungsten filament at a residual pressure of 10^{-7} Torr. Aluminum is chosen because it adheres well to the rather inert GaSe surface. The GaSe flakes are then bonded with 100% solids, silver-loaded epoxy to a brass block of convenient dimensions. The exposed surface of the GaSe film is thereafter peeled away by successive application and removal of Scotch transparent tape (3M# 810). Care is taken to peel off a continuous film of GaSe thereby avoiding possible contamination of the GaSe surface with adhesive from the tape. As the film thins, interference colors become visible. With continued peeling, the film becomes too thin to generate interference colors. At this juncture, it is, of course, not at all clear to the experimenter that any film remains. The specimen is then again placed in the vacuum system and gold or copper counter electrode is evaporated onto the freshly exposed GaSe surface. A fine wire mesh is used to define a regular array of square dots, 4.5×10^{-5} cm^2 in area, as counter electrodes. The specimen is now complete and ready for preliminary testing to determine if it con-

$$\left[\begin{array}{c} \dfrac{\delta \mathcal{L}}{\delta K(\xi)} = \displaystyle\int_\alpha^\beta \Gamma\, dE \\ \Gamma(V,\xi,E) = \dfrac{e}{2\pi\hbar\zeta}\left[2 - \dfrac{(\phi_2-\phi_1-V)}{t}\left(\dfrac{1}{k^2(\xi)\,\zeta}\right)\right] \exp\left\{\dfrac{-2t}{\phi_2-\phi_1-V}\displaystyle\int_{\phi_1+E}^{\phi_2+E-V} k(\xi')\,d\xi'\right\} \\ \zeta = \displaystyle\int_{\phi_1+E}^{\phi_2+E-V_1} \dfrac{d\xi'}{k(\xi')} \end{array}\right]$$

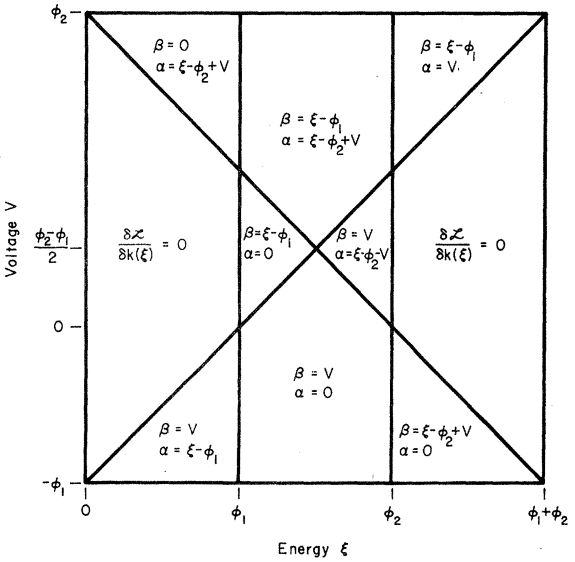

FIG. 2. Functional derivative $d\mathcal{L}/dk(\xi)$, used in the calculation of the energy-momentum dispersion relation from appropriate experimental current-voltage data, is shown along with a diagram of the plane in voltage-energy space over which this functional derivative is to be evaluated.

tains MIM structures of appropriate and uniform thickness.

C. Preliminary Calculations

The properties of the single-crystal GaSe film incorporated within metal-GaSe-metal structures are known, and hence the shape of the potential barrier presented by this insulating film may be calculated. In the first approximation, the barrier potential may be taken to be trapezoidal, as shown in the inset to Fig. 4:

$$\phi(x) = \phi_1 + (\phi_2 - \phi_1 - eV)\, x/t \,. \tag{3.1}$$

The presence of space charge in the GaSe layer, and the effect of image charges induced in the electrodes, may lead to the deviation of the barrier shape from the assumed trapezoidal form.

Space charge distorts the shape of the potential barrier because field lines originate or terminate on the trapped charge. Using the worst case assumption that all traps are ionized and assuming that the space charge is distributed uniformly throughout the barrier region, integration of Poisson's equation yields a modification to the barrier ($\Delta\phi = eN_t t^2/2\epsilon$) which is less than 10^{-3} eV, and thus, is totally negligible.

Electrons tunneling through the GaSe layer interact with electrons in the two metallic electrodes. This interaction can be modeled by adding, to the expression for a trapezoidal barrier potential, the potential due to image charges which one would expect (in the classical approximation) to be induced in the electrodes. However, for typical values of the parameters of a GaSe structure (thickness equal to 70 Å, dielectric constant equal to 8) the error introduced in the E-k relation by neglecting this modification to the barrier shape is small (estimated to be less than 0.015 Å^{-1} for the E-k relation derived from forward-bias currents).

Being now assured that the actual potential barrier within metal-GaSe-metal structures is well approximated by the simple trapezoidal model, we can make an estimate of the conditions under which direct interelectrode tunneling is likely to be the dominant mechanism of current flow. Bulk limitations have been shown[28] to be negligible even for 600-Å films, and hence can be neglected here. Thermionic currents have an exponential dependence on barrier height and temperature[28]

$$J_{\rm th} = J_0 e^{-\phi/k_B T} \,, \tag{3.2}$$

where $J_0 \approx 120T^2$ amp/cm^2 and k_B is Boltzman's constant. Tunneling probability (and hence tunneling current) increases exponentially with decreasing tunneling path length[10]

$$J_T = J_0' e^{-2kt} \,, \tag{3.3}$$

where $\hbar^2k^2/2m^* = E$ (parabolic band approximation) and

$$J_0' = \frac{e}{8\pi h}\frac{\phi}{t^2} \simeq 1.5\times 10^{-6}\frac{\phi[\text{eV}]}{t^2[\text{cm}^2]} \quad \frac{\text{amp}}{\text{eV}} \,.$$

Assuming $\phi \simeq 0.6$ eV and $t \simeq 10^{-6}$ cm, $J_0' \simeq 10^6$ amps/cm^2. Tunneling will be the dominant mechanism of current flow if $J_T > J_{\rm th}$, i.e.,

$$J_0' e^{-2kt} \gg J_0 e^{-\phi/k_B T} \,. \tag{3.4}$$

This expression is a condition on both t and T. Since the thickness dependence of the tunneling probability is its most striking feature, it is worthwhile working at as low a temperature as possible, thus extending the thickness range over which tunneling is the dominant current-flow mechanism. The lowest barrier with which we are concerned is $\phi_{\rm Au} \simeq 0.5$ eV. Taking $k \simeq 0.4$ Å^{-1} ($E = \frac{1}{2}$ eV, $m^* = 1$) as a rough estimate, tunneling is thus expected to dominate for $t \ll 100$ Å at 77 °K and for $t \ll 30$ Å at 300 °K.

D. Measurement Technique

An important experimental question is the temperature at which current-voltage measurements are to be made. Room ambient is convenient, but the interface barrier energies in GaSe structures are sufficiently low that thermionic currents are expected to be dominant except in extremely thin structures, thus unduly restricting the thickness range over which measurements can be taken. Liquid-helium temperatures are ideal for eliminating thermionic currents, but the inability to temperature-cycle GaSe MIM structures without mechanically destroying them, and the need to sample many structures to assure reliable data, make working in this temperature range extremely difficult.

As a workable compromise between the limitations of room-temperature and liquid-helium environments, a measurement technique for use at liquid-nitrogen temperature was evolved. The specimen bearing substrate is entirely immersed in liquid nitrogen after fabrication, and remains immersed through the entire measurement process. Viewing of the specimens to locate suitable individual structures for probing (with a fine gold wire) and measurement is accomplished with a specially constructed "under-nitrogen viewer." This viewer[29] is an evacuated thin-walled stainless-steel conical tube fitted with sapphire windows at either end. The thermal conductivity of this viewer is sufficiently small that one end can be immersed under the surface of a liquid-nitrogen bath, and permit viewing of objects therein, without excessive bubbling or boil-off and without frosting at the exposed end. With this viewer a given specimen could be probed for a period of several hours, and many structures investigated. Care was taken to choose a fine springy probe wire

with a rounded top to avoid mechanically damaging the structure under test.

E. Selection of Structures

Preliminary measurements consist of determining the capacitance of each MIM structure on a given substrate to ascertain which structures have insulator thickness within the interesting (< 100 Å) range. Questions of insulator uniformity, the validity of the trapezoidal-barrier approximation, and the dominance of tunneling as the mechanism of current flow, must be answered before detailed analysis is undertaken. These questions are coupled and may be simply resolved. Assuming the simple trapezoidal-barrier model (Fig. 1) with an arbitrary E-k relation in the forbidden gap of the insulator, the simple ideas of an exponentially damped wave function lead to a tunneling probability which decreases exponentially with increasing tunneling path.[3] Near zero bias, the tunneling probability is inversely proportional to the tunneling time RC and is given by[10]

$$RC = (2\pi\epsilon h/e)[1/\bar{k}(\xi)]\, e^{2t\bar{k}(\xi)} . \qquad (3.5)$$

Hence, near zero bias the natural logarithm of RC should depend linearly on insulator thickness t with proportionality constant $2\bar{k}(\xi)$ where $\bar{k}(\xi)$ is the average value of k encountered in the tunneling path corresponding to an incident electron with zero transverse momentum and energy equal to the metal Fermi energy. Therefore, experimental observation of a zero-bias tunneling time which is exponentially proportional to insulator thickness t is good evidence that tunneling is the dominant mechanism of current flow and that the trapezoidal-barrier model is appropriate.

In addition to a tunneling time experimentally proportional to insulator thickness, the zero-thickness intercept of this plot should be within an order of magnitude of $(2\pi\epsilon h/e)\,(1/\bar{k}) \simeq 10^{-15}$ sec. Major deviations from this value require further investigation. Having thus identified (by simple measurements performed on the structure under study) tunneling through a trapezoidal barrier as the mechanism of current flow, this technique can be refined and used to select uniform-thickness structures from the multitude incorporating an insulating film of nonuniform thickness (i.e., those having cleavage steps).

Consider the physical situation. The experimental specimens consist of nominally 5–20 layers of GaSe. A cleavage step of one or more layers will drastically affect the spatial distribution of current under a given counterelectrode since current flow via tunneling is exponentially weighted toward thinner films. However, the apparent thickness, as determined from capacitance measurements, is weighted only linearly by thickness variations. Hence, for every apparent thickness it is possible to observe RC time constants substantially below that corresponding to a uniform insulator thickness. Clearly, a specimen selection technique is required to prevent a morass of confusing and self-contradictory data from being subjected to detailed analysis. The technique is simple. One merely selects those samples bounding the experimental half-plane of $\ln RC$-vs-t measurements. A large number of specimens must be examined, but if tunneling is indeed the mechanism of current flow, a well-defined bounding line will eventually emerge.[30] If this line is indeed straight, and its intercept of the expected magnitude, then the trapezoidal-barrier assumption may be assumed valid (particularly if calculations of the expected barrier shape, using the known parameters of the bulk material from which thin-film structures are fabricated, predict this simple barrier shape, as is the case for metal-GaSe-metal structures).

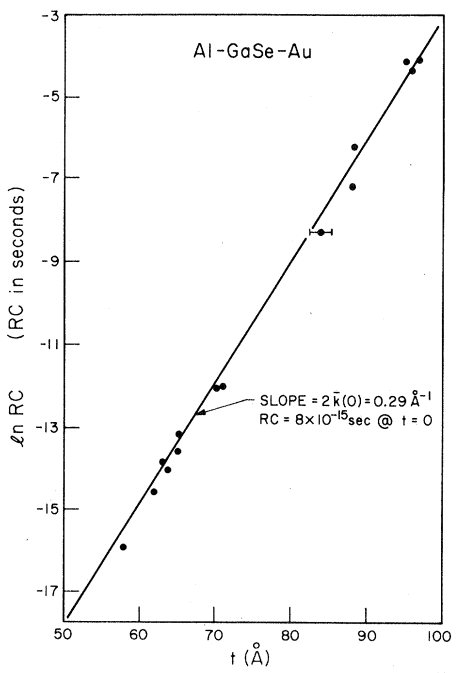

FIG. 3. Plot of $\ln RC$ (measured near zero bias) vs apparent thickness t (as calculated from measured structure capacitance). Only data for those structures with the largest experimentally observed RC time constant is shown for each apparent thickness. These data correspond to structures having the most nearly uniform insulating layers, as explained in the text. Since a straight line is a good fit to the data, direct interelectrode tunneling is indicated as the dominant conduction mechanism. Typical error bar, shown on one data point, corresponds to the scatter in counter-electrode area, as measured photographically.

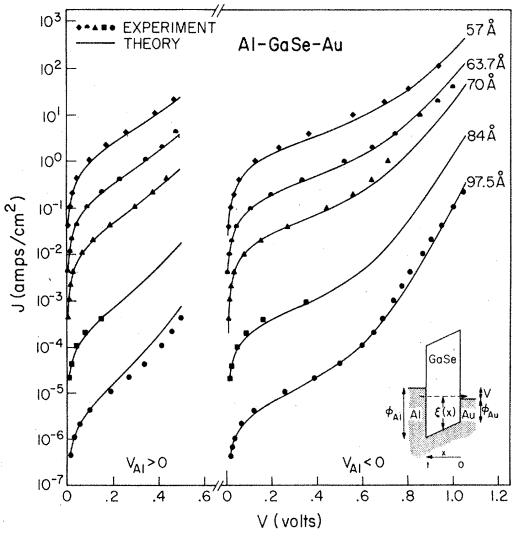

FIG. 4. Current-voltage curves, for both directions of applied bias, of a number of Al-GaSe-Au structures. Solid symbols represent experimental data obtained on structures whose apparent thickness was calculated directly from the measured structure capacitance. Theoretical curves (solid lines) were calculated from the E-k relation of Fig. 5, the known properties of GaSe, and from the tunneling model of Sec. II [Eq. (2.11)]. Agreement between theory and experiment is seen to be very good. Inset to this figure shows the schematic energy-band representation of Al-GaSe-Au structures.

IV. RESULTS AND INTERPRETATION

A. Al-GaSe-Au Structures

Figure 3 shows the zero-bias time constant of a selection of Al-GaSe-Au structures plotted vs apparent GaSe thickness (as determined from capacitance measurements). The data shown was obtained from those specimens of highest resistance and hence of most nearly uniform insulator thickness. These data form a straight line over a wide thickness range, and hence direct tunneling through a trapezoidal barrier is indicated as the dominant mechanism of current flow. The slope of this straight line gives a good estimate of $\overline{k}(\xi)$ as indicated by Eq. (3.5). The error bar shown on one data point is representative of the error in apparent thickness arising from scatter in the actual area of individual counter electrodes as formed in the specimen fabrication process. This random error is the most important uncertainty in this series of experiments since the thickness enters calculated currents in the exponent.

Figure 4 presents detailed current-voltage data obtained on structures of uniform thickness (selected according to the procedure discussed in the previous section; see also Fig. 3). Data was obtained over that voltage range, for each bias direction, for which direct interelectrode tunneling is possible. This voltage range ($V<\phi_1$, $V<\phi_2$; see insert to Fig. 4) is known *a priori* since the metal-GaSe interface barrier energies are known from prior experiments on bulk specimens. The data of Fig. 4 (solid symbols) correspond to structures ranging over 57–97 Å in insulator thickness. The data of Fig. 4 were used as input to the numerical inversion program discussed in Sec. II to obtain approximate E-k curves for GaSe. Inversion of the I-V curve for each thickness yields an E-k curve. These E-k curves were extremely similar and hence were averaged to obtain an overall best-fit E-k curve, shown in Fig. 5. This energy-momentum dispersion relation is parabolic near the valence band, as expected, and departs from parabolicity toward midgap. The implications of this E-k curve are discussed below, after its accuracy has been established.

The theoretical I-V curves in Fig. 4 were calculated directly from the E-k curve of Fig. 5, the known parameters of GaSe (Sec. III), and the simple tunneling theory of Sec. II as represented

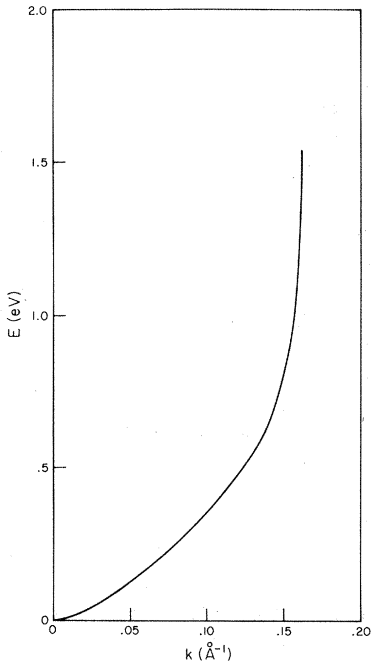

FIG. 5. Experimentally determined energy-momentum dispersion relation within the forbidden gap of GaSe. This relation is an average of the E-k relations determined by numerically inverting each experimental I-V curve of Fig. 4. Since only that portion of the E-k relation from the valence band up to $\phi_1+\phi_2$ is active in determining the tunneling currents within a given MIM structure, the use of aluminum and gold as electrodes limits the range over which $E(k)$ may be calculated to that shown (i.e., $\phi_{Al}+\phi_{Au}\simeq 1.5$ eV). This relation is parabolic near the valence band, as expected, but possesses rather little curvature for $E>0.6$ eV.

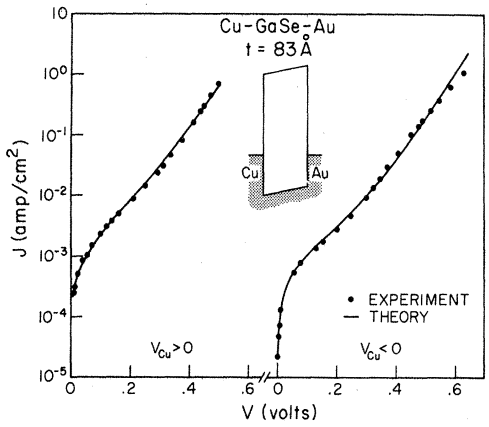

FIG. 6. Experimental current-voltage curve of an 83-Å (as determined directly from the measured capacitance) Cu-GaSe-Au structure is shown by the solid symbols. The solid curve is calculated from the E-k relation of Fig. 5, the known properties of GaSe, and the tunneling model of Sec. II [Eq. (2.11)]. Agreement between theory and experiment is excellent thereby indicating that the previously determined E-k relation is intrinsic to GaSe. Inset shows a schematic energy-band representation of the Cu-GaSe-Au structure.

by Eq. (2.11). The exceptionally good agreement between theory and experiment as illustrated by Fig. 4 is evidence that the model of Sec. II is adequate to describe tunneling in Al-GaSe-Au structures, since the E-k curve is highly over specified by the data. That is, each I-V curve contains enough information to uniquely define the E-k relation over the relevant portion of the forbidden gap. The observation of quantitative agreement between current-voltage curves measured for a wide range of insulator thickness, and theoretical predictions based on a single E-k relation, indicates a complete self-consistency of the theoretical model with the experimental situation. As a consequence, we are well assured at this point that direct interelectrode tunneling is the dominant mechanism of current flow in Al-GaSe-Au structures and that a single E-k dispersion relation accurately describes the tunneling phenomenon over a wide range of insulator thickness. Further experiments are required to assure that the E-k relation thus far obtained is an intrinsic and fundamental property of GaSe.

B. E-k Dispersion Relation

A crucial test of the validity (as indeed a fundamental and accurately determined property of GaSe) of the E-k relation of Fig. 5 is the quantitative prediction of tunneling currents in structures other than the Al-GaSe-Au ones from which this relation was determined. For example, a tunneling electron in a Cu-GaSe-Au structure encounters a range of k for each applied bias which is quite different from that in an Al-GaSe-Au structure. As may be seen in the inset of Fig. 6, the band diagram of a Cu-GaSe-Au structure is distinguished from that of an Al-GaSe-Au structure by the low 0.4-eV Cu-GaSe barrier energy.

The known properties of GaSe in conjunction with the E-k relation of Fig. 5 are, as previously discussed, adequate to permit calculation of the tunneling current-voltage curves to be expected in Cu-GaSe-Au structures. The result of such a calculation (as in Sec. II, with no adjustable parameters of any sort) is shown in Fig. 6 along with data obtained on an experimental structure. The thickness used in this calculation is (as throughout this paper) determined directly from the measured capacitance of the experimental structure. The agreement between theory and experiment, shown in Fig. 6, is excellent evidence that the E-k relation previously determined for GaSe is a fundamental and intrinsic property of GaSe.

The accuracy to which the energy-momentum dispersion relation of GaSe has been determined in this series of experiments may also be gauged by the comparison, presented in Fig. 7, between the experimentally determined E-k curve and a common analytic approximation (Franz's two-band model: $m_v^* = 0.07$, $m_c^* = 0.35$). The inset shows that the experimentally determined E-k relation (solid line) and the two-band approximation differ only slightly. Yet the experimental I-V curve (solid circles) is seen to be in distinctly better agreement with the predictions of the actual E-k curve than with those of the approximation.

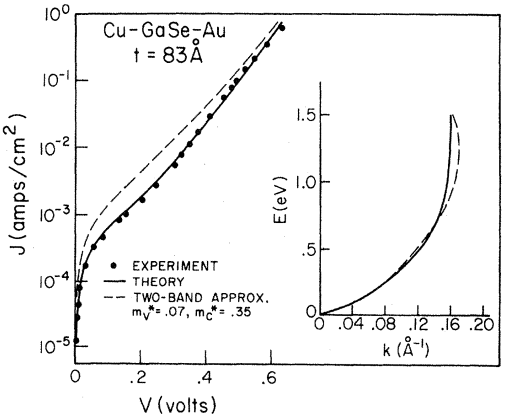

FIG. 7. Figure presents both the experimentally determined E-k relation of GaSe, and also a common two-parameter approximation (Franz's two-band model), and compares the tunneling currents predicted by each. Sensitivity of the J-V curve to small changes in the E-k relation may be gauged by comparison of the deviation between the two $E(k)$ curves and the corresponding $J(V)$ curves.

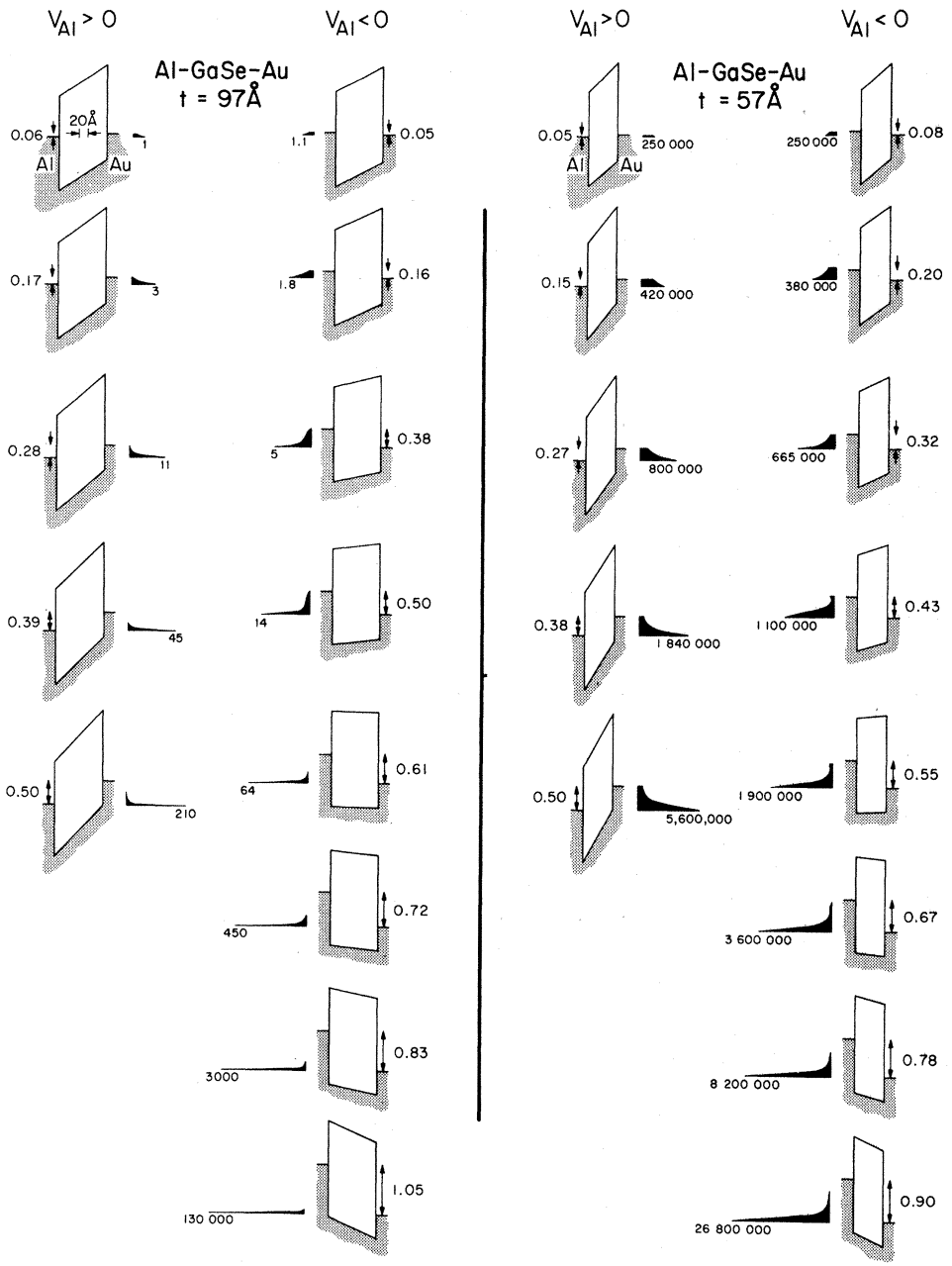

FIG. 8. Energy distributions of tunneling electrons and corresponding band diagrams for two Al-GaSe-Au structures. Distributions were calculated using the techniques of Sec. II and give insight into the origin of tunneling current. All distributions are plotted on linear scales so that a visual estimate of the width of the distribution is meaningful. The number beneath the peak of each distribution indicates the absolute magnitude of that peak relative to the peak of every other distribution in the figure. For the 97-Å structure, the width of the distribution (shaded curve) diminishes rapidly with increasing applied bias. However, for the 57-Å structure rather broad tunneling distributions are noted at all bias values. This distinction occurs because the thicker the sample, the more strongly the current distribution is weighted toward low values of k. The lack of appreciable curvature in the $E(k)$ relation for $E > 0.6$ eV (see Fig. 5) gives rise to unusually broad tunneling distributions near zero bias, even for relatively thick specimens of GaSe.

C. Energy Distribution of Tunneling Electrons

Having at our disposal an accurate E-k relation, the physics of electron tunneling may be more fully appreciated by using the previously discussed computer program to numerically calculate the energy distributions of tunneling electrons.

Energy distributions of tunneling electrons are

shown for several values of applied bias in Fig. 8. These distributions have been calculated for Al-GaSe-Au structures having thicknesses at the extremes of the range studied; the calculations span the range of biases over which direct interelectrode tunneling is possible. For reference, a band diagram is shown for each bias condition. The number beneath each distribution (solid curve) is the relative magnitude of the peak of that distribution. Each distribution is drawn on a linear scale so that a visual estimate of its width will be meaningful.

Considering first the thicker (97-Å) structure, it is clear that the nearly flat part of the E-k curve (see Fig. 5, $E > 0.6$ eV) leads to rather broad tunneling electron distributions at low bias. However, as the bias is increased the relevant portion of the E-k curve is extended toward $E = 0$ and hence the tunneling distribution becomes very peaked about the source-electrode Fermi level. This peaking is exactly what is expected because the exponential damping of the electronic wave function heavily weights the transmitted distribution toward small values of k. At small insulator thicknesses, however, the weighting toward low k is correspondingly less. Therefore, in thin structures, electrons at all possible energies contribute to the tunneling current, even at high bias. The degree to which this contribution is significant depends, in general, on the curvature of the E-k relation. For GaSe, this curvature is rather small for large energy, and consequently, electron tunneling through midgap can be a major contribution to the total current.

It is interesting to note that the approximation technique of Stratton *et al.*[12] which is based on a distribution of carriers sharply peaked about the Fermi level of the source electrode would have been inadequate and inappropriate for the calculation of tunneling currents in GaSe. This conclusion could have been inferred from the lack of self-consistency which would have resulted had that approach been used,[31] but may be directly drawn from Fig. 8. The numerical technique of Sec. II includes all contributions to the total tunneling current and hence is more general than the technique of Stratton *et al.*[12] in the sense that no assumption need be made about the nature of the E-k curve.

V. CONCLUSIONS

We have studied current flow in MIM structures incorporating single-crystal films of GaSe less than 100 Å thick. The dominant mechanism of current flow in these structures is direct interelectrode tunneling through a trapezoidal potential barrier. Identification of this mechanism is based on quantitative comparison between experimental data and theoretical predictions calculated from the known properties of bulk GaSe.

The E-k dispersion relation within the forbidden gap of GaSe was calculated from a small subset of the data obtained and is shown to be intrinsic to GaSe. Knowledge of this relation, the properties of the bulk insulator, and the geometry of a given structure are sufficient to quantitatively predict tunneling currents and their dependence on applied bias, insulator thickness, and metal-insulator barrier energy. We therefore conclude that a single one-electron model of tunneling is an appropriate and sufficiently accurate description of current flow in those physical situations where the criteria for its applicability are fulfilled. These criteria are straightforward and can be examined *a priori* if the structure under study is well defined and the relevant electronic properties of its constituents are known.

Tunneling measurements provide a direct technique for measuring the energy-momentum dispersion relation within the forbidden gap of an insulator. This relation represents fundamental information about a given solid which cannot be obtained by other methods.

---

†Work supported in part by the Office of Naval Research.

*Hertz Foundation Doctoral Fellow.

‡Howard Hughes Doctoral Fellow.

[1]A. Sommerfeld and H. Bethe, *Handbuch der Physik von Geiger und Scheel* (Springer-Verlag, Berlin, 1933), Vol. 24/2, p. 450ff.

[2]C. B. Duke, *Tunneling in Solids* (Academic, New York, 1969).

[3]C. A. Mead, *Tunneling Phenomena in Solids* (Plenum, New York, 1969), Chap. 9.

[4]R. M. Handy, Phys. Rev. 126, 1968 (1962).

[5]J. C. Fisher and I. Grover, J. Appl. Phys. 32, 172 (1961).

[6]G. T. Advani *et al.*, Proc. IRE 50, 1530 (1962).

[7]D. Meyerhoffer and S. A. Ochs, J. Appl. Phys. 34, 2535 (1963).

[8]R. Holm, J. Appl. Phys. 22, 569 (1951).

[9]M. McColl and C. A. Mead, Trans. Met. Soc. AIME 233, 502 (1965); M. McColl, Ph. D. thesis (California Institute of Technology, 1964) (unpublished).

[10]G. W. Lewicki and C. A. Mead, Phys. Rev. Letters 16, 939 (1966).

[11]G. W. Lewicki and C. A. Mead, J. Phys. Chem. Solids 29, 1255 (1968).

[12]R. Stratton, G. Lewicki, and C. A. Mead, J. Phys. Chem. Solids 27, 1599 (1966).

[13]J. Bardeen, Phys. Rev. Letters 6, 57 (1961).

[14]M. H. Cohen, L. M. Falicov, and J. C. Phillips, Phys. Rev. Letters 8, 316 (1962).

[15]*Tunneling Phenomena in Solids*, edited by E. Burstein and S. Lundqvist (Plenum, New York, 1969).

[16]W. A. Harrison, Phys. Rev. 123, 85 (1961).

[17]T. C. McGill, Ph. D. thesis (California Institute of

Technology, 1969) (unpublished).

[18]V. Heine, Proc. Phys. Soc. (London) 81, 300 (1963).

[19]E. I. Blount, *Solid State Physics* (Academic, New York, 1962), Vol. 13, Appendix C.

[20]E. T. Copson, *Asymptotic Expansions* (Cambridge U. P., Cambridge, England, 1965).

[21]Hence, the error caused by this assumption can be estimated only after an E-k curve is computed and the actual energy distribution of tunneling electrons is available.

[22]ϕ_1 is taken to be less than ϕ_2.

[23]H. A. Antosiewicz and W. C. Rheinboldt, *Survey of Numerical Analysis* (McGraw-Hill, New York, 1962), Chap. 14, pp. 512–514.

[24]Numerical techniques used in this calculation are more fully discussed in Ref. 17.

[25]J. Franklin, J. Math. Anal. Applications 30, (1970).

[26]D. P. Foote and B. Kazan, Report No. ASO-TDR-63-640, 1963 (unpublished).

[27]P. Fielding, A. Fisher, and E. Mooser, J. Phys. Chem. Solids 8, 434 (1959); J. L. Brebner, *ibid.* 25, 1427 (1964); R. H. Bube and E. L. Lind, Phys. Rev. 115, 1159 (1959).

[28]T. C. McGill, S. Kurtin, and C. A. Mead, J. Appl. Phys. 41, 3831 (1970).

[29]The assistance of M. Simpson in the fabrication of this viewer is gratefully acknowledged.

[30]As a practical matter, a well-prepared substrate may contain several small regions of 5–15 structures each with nearly the same capacitance. Experience indicates that such a region contains, at its center, structures whose insulator thickness is uniform.

[31]This sort of inconsistency was noticed by Lewicki [G. W. Lewicki, Ph. D. thesis (California Institute of Technology, 1966) (unpublished); available from University microfilms, Ann Arbor, Michigan] in his study of AU-AlN-Al structures and attributed to wide tunneling distributions. The techniques discussed herein have been applied to Lewicki's data with notable success (see Ref. 17).

PHYSICAL REVIEW B VOLUME 3, NUMBER 10 15 MAY 1971

Mobility of Hot Electrons in n-Type InAs

R. C. Curby and D. K. Ferry
Department of Electrical Engineering, Texas Tech University, Lubbock, Texas 79409

(Received 26 October 1970)

A detailed study of the change in hot-electron mobility with applied electric fields in n-type InAs at 77 °K is presented. Both theoretical and experimental results are presented. Electron-electron collisions are assumed to be sufficiently frequent to determine the energy and momentum distribution of the electrons. The effects of ionized-impurity scattering are included in the momentum balance equation. The nonparabolicity of the conduction band is included in the theoretical calculation. The effect of the overlap integral which results in the nonparabolicity is included in the manner of Ehrenreich by utilizing several terms of the scattering matrix element. For low electric field (< 150 V/cm), a slight increase (approximately 10%) in the mobility with applied electric field is observed. For higher electric fields (> 150 V/cm), a strong decrease in the mobility with applied electric field occurs. This decrease is observed up to the point of impact ionization at approximately 800 V/cm.

INTRODUCTION

The mobility of hot electrons in polar semiconductors has become of interest in recent years with the production of III-V and II-VI compounds in relatively pure form. Most of the past work in III-V compounds has been for indium antimonide (InSb) and gallium arsenide (GaAs). For indium arsenide (InAs), some of the theories which have been applied to InSb can be used, since these materials have approximately the same band structure. In the present work, we calculate the transport properties for n-type InAs at 77 °K for applied electric fields below that required for the onset of impact ionization. There have been a few theories for InSb developed by using various approaches, and some of these may be, or have been, applied to InAs.

One of the earliest theories for InSb was presented by Ehrenreich.[1] He was one of the first to include the nonparabolicity of the energy band, doing so with the theory of Kane.[2] Kane's theory results from taking the interaction of the valence bands and the conduction band through the $\vec{k}\cdot\vec{p}$ terms of the Hamiltonian. The $\vec{k}$-independent spin-orbit interaction is also taken into account exactly. This refinement was necessary because the narrow band gap in these materials makes these interactions too strong for perturbation theory to yield accurate results. From these calculations, the relation between the energy bands $\mathcal{E}(\vec{k})$ and the crystal momentum $\hbar\vec{k}$ is no longer a simple parabolic relation, but is more nearly hyperbolic. Ehrenreich confined his calculation to temperatures above 200 °K to avoid problems arising from crystalline imperfections, such as ionized impurities.